ACS APPLIED MATERIALS & INTERFACES

www.acsami.org Research Article

Green Synthesis of Oxide-Supported Pd Nanocatalysts by Laser Methods for Room-Temperature Carbon–Carbon Cross-Coupling Reactions

Mrinmoy K. Das, Julian A. Bobb, Amr A. Ibrahim, Andrew Lin, Khaled M. AbouZeid, and M. Samy El-Shall*

Cite This: *ACS Appl. Mater. Interfaces* 2020, 12, 23844–23852 Read Online

ABSTRACT: This work reports the design and development of a new class of highly active Pd nanocatalysts supported on substoichiometric oxides. These novel catalysts are generated by green laser synthesis methods to generate high-surface-area substoichiometric oxide nanoparticles followed by photoreduction in aqueous solutions to deposit highly active Pd nanocatalysts within the surface defects of the oxides. The laser methods eliminate the use of toxic chemicals, including hazardous solvents and chemical reducing agents, and allow efficient reduction of the Pd ions in aqueous solutions aided by the photogenerated electrons from the semiconductor support. The Pd catalysts incorporated within these oxides exhibit high activity for carbon–carbon bond-forming reactions. The Pd/TiO_2 catalyst with 0.3 mol % Pd achieves 100% conversion in the reaction between bromobenzene and benzeneboronic acid to the biphenyl product within 240 minutes at room temperature without any external heating. With a catalyst loading of 0.3 mol % Pd in the microwave-assisted reaction between bromobenzene and benzeneboronic acid at 60 °C, 92 and 83% conversions to the biphenyl product are achieved within 5 min of reaction time using the Pd/TiO_2 and Pd/ZnO catalysts, respectively. The results demonstrate a remarkable catalytic activity of the substoichiometric oxide-supported Pd catalysts with turnover frequencies (TOF, h^{-1}) of 24 000, 10 000, and 3200 achieved under mirowave-assisted reactions at 60 °C for the 0.03 mol% Pd of the Pd/TiO_2, Pd/ZnO, and Pd/ZrO_2 catalysts, respectively. The high activity and good reusability of these nanocatalysts are attributed to the optimum catalyst–support interaction between the small Pd nanoparticles and the surface defects of the substoichiometric oxide support prepared by the laser vaporization-controlled condensation method.

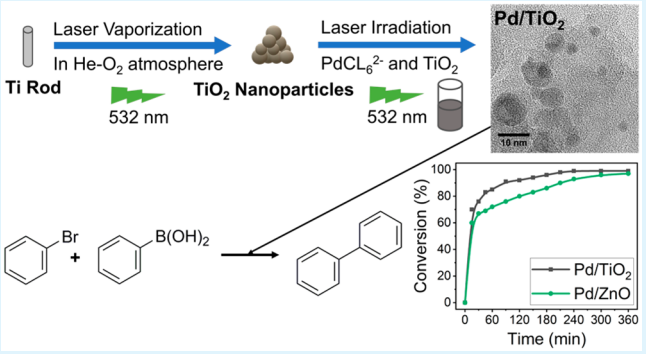

KEYWORDS: *laser vaporization-controlled condensation, laser photoreduction, substoichiometric oxide nanoparticles, supported Pd nanocatalysts, Suzuki coupling reactions*

1. INTRODUCTION

Palladium-catalyzed carbon–carbon cross-coupling reactions are of strategic importance in the synthesis and assembly of functionalized complex organic molecules.[1−6] Organic molecules with greater chemical complexity are particularly needed for the development of pharmaceuticals and drug discovery.[7−9] These molecules used in active pharmaceutical ingredients (APIs) are typically synthesized using Pd-catalyzed homogeneous reactions and utilizing ligands to enhance the activity and selectivity.[1−9] However, these processes lead to residual metal that contaminates the reaction product.[9,10] This is a major issue particularly in pharmaceutical applications where this chemistry is extensively used, since palladium compounds can be highly toxic. Coupled with the difficulty to recycle the metal as well as the ligand results in a significant cost component in API applications.[10] The development of supported catalysts that could reduce/eliminate leaching and sintering, enhance performance, and could also be recycled would be a significant step in lowering the cost of the synthesis of chemicals and drugs. Understanding the role of the support in the Pd-catalyzed reactions is an important step toward optimizing the activity of the supported catalysts and the development of more effective and less expensive catalysts for chemical and pharmaceutical industries.[9−14]

Received: February 20, 2020
Accepted: April 28, 2020
Published: April 28, 2020

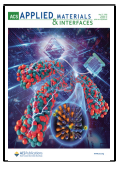

https://dx.doi.org/10.1021/acsami.0c03331
ACS Appl. Mater. Interfaces 2020, 12, 23844–23852

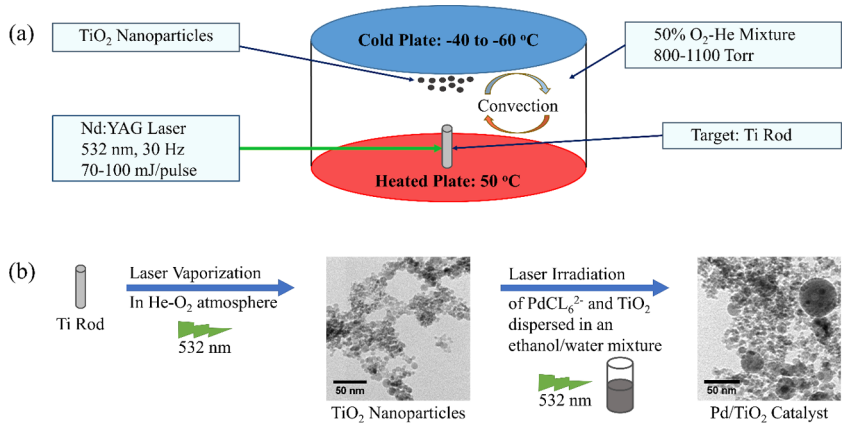

Figure 1. (a) Schematic illustration of the synthesis of TiO_2 nanoparticles by the LVCC method from using a Ti rod. (b) Schematic illustration of the LIS method for the deposition of Pd nanoparticles on the TiO_2 support.

A variety of oxide-based supports such as TiO_2,[13,15−20] ZrO_2,[21] ZnO,[22] and SiO_2[18,23−25] have been utilized for mobilizing Pd nanoparticles for cross-coupling reactions. In oxide-supported Pd catalysts, both electron and O atom transfers at the active metal and oxide support interface can improve the catalytic activity; however, if the metal−support interaction (MSI) is poor, the Pd metal can leach significantly into the solution.[1,26,27] A strong MSI could also help in the homogeneous dispersion of the catalyst and prevents the aggregation of active metal nanoparticles on the oxide support. Structural defects such as oxygen vacancies in the non-stoichiometric oxide support could enhance MSI by providing preferred nucleation sites for the Pd nanoparticle catalysts. In addition, laser photochemical reduction of the Pd precursor ions adsorbed on the surface of the oxide support could generate further defects and incorporate the Pd nanoparticles within these defects. For metal oxide supports with band gaps accessible by laser irradiation in solution, the photogenerated electrons can aid the reduction of the Pd ions and reduce or eliminate the need for hazardous reducing agents and high temperatures, thereby allowing a good control of the reduction process.

In this work, we introduce a new strategy for the synthesis of nonstoichiometric metal oxide supports and the deposition of highly active Pd nanocatalysts on these supports using a combination of the laser vaporization-controlled condensation (LVCC) and the laser irradiation in solution (LIS) techniques. These laser methods eliminate the use of toxic chemicals, including hazardous chemical reducing agents and solvents, and allow efficient reduction of the Pd ions in aqueous solutions assisted by the photogenerated electrons from the semiconductor support. The combined LVCC−LIS techniques presented here provide a green synthesis route of the oxide-supported Pd nanoparticle catalysts, which exhibit high activity and good recyclability for carbon−carbon bond-forming reactions.

2. EXPERIMENTAL SECTION

2.1. Materials. Ti, Zr, Zn, and Si rods were obtained from Sigma-Aldrich. Potassium hexachloropalladate(IV) (K_2PdCl_6; Pd 26.3% min) and hydrazine hydrate (N_2H_4, reagent grade) were obtained from Alfa Aesar, and ethyl alcohol (200 proof absolute, anhydrous, ACS/USP grade) was purchased from Pharmco-Aaper.

2.2. Synthesis of Pd/Oxide Catalysts by LIS. A K_2PdCl_6 stock solution was prepared by adding 0.235 mg of K_2PdCl_6 to a mixture of 10 mL of ethanol and 10 mL of water and sonicated/stirred for 24 h until full dispersion of the palladium salt. Afterward, the solution was diluted to 25 mL. The TiO_2, ZrO_2, ZnO, or SiO_2 nanoparticles were immersed in 1:1 ethanol/water and sonicated/stirred until complete dispersion. The required amount of the K_2PdCl_6 (1.2 mL) stock solution was then added to the dispersed TiO_2, ZrO_2, ZnO, or SiO_2 solution (60 mg support in 4.8 mL of 1:1 ethanol/water mixture). The solution was stirred for 24 h to ensure homogeneous dispersion. The solution (6 mL) was then irradiated with a Nd:YAG laser (532 nm, 4 W, 30 Hz) for 12 min under stirring. The precipitate was washed by centrifugation with ethanol and dried overnight at 80 °C. These catalysts are denoted as LIS-Pd/TiO_2, LIS-Pd/ZrO_2, LIS-Pd/ZnO, or LIS-Pd/SiO_2, respectively.

2.3. Synthesis of Pd/Oxide Catalysts by MW-Assisted Chemical Reduction. Pd nanoparticles were deposited on the TiO_2, ZrO_2, ZnO, or SiO_2 support by the microwave-assisted chemical reduction method using hydrazine hydrate as a reducing agent. The required amount of the K_2PdCl_6 stock solution (1.2 mL) was added to the dispersed TiO_2, ZrO_2, ZnO, or SiO_2 solution (60 mg of support in 4.8 mL of 1:1 ethanol/water mixture). The solution was stirred for 24 h to ensure homogeneous dispersion. A small quantity of the hydrazine hydrate reducing agent (0.3 mL) was then added, and the solution was immediately transferred to a microwave oven and irradiated for 30 s with 1000 W microwave irradiation (MWI). The precipitate was then washed with ethanol and dried overnight at 80 °C. These catalysts are denoted as MW-Pd/TiO_2, MW-Pd/ZrO_2, MW-Pd/ZnO, or MW-Pd/SiO_2, respectively.

2.4. Procedure for Suzuki Cross-Coupling Reactions at Room Temperature. The as-prepared catalysts were characterized and applied in the Suzuki cross-coupling reaction of bromobenzene and phenylboronic acid. Bromobenzene (50 mg, 0.32 mmol, 1 equiv) and phenylboronic acid (47 mg, 0.38 mmol, 1.2 equiv) were mixed into an ethanol (2 mL)/water (2 mL) solution. The required amount of catalyst (0.3 mol % Pd) was dispersed, followed by the addition of 133 mg of K_2CO_3 (0.96 mmol, 3 equiv). The reaction proceeded at room temperature over the course of 8 h with intermittent sampling. The sample was extracted using centrifugation and ethyl acetate. Gas chromatography-mass spectrometry (GC-MS) was utilized to identify the reactant and product peaks, and GC−flame ionization detection (FID) was used to determine the ratio of bromobenzene (limiting reactant) and biphenyl (product) to determine the % conversion. The % conversion to the biphenyl product was calculated using the GC-FID data as follows: [(product peak area)/(reactant peak area + product peak area)] × 100.

2.5. Procedure for Suzuki Coupling Reactions under Microwave Irradiation (MWI). The Suzuki cross-coupling was also performed under MWI using different Pd catalyst concentrations. Bromobenzene (50 mg, 0.32 mmol, 1 equiv) and phenylboronic acid (47 mg, 0.38 mmol, 1.2 equiv) were added to an ethanol (2 mL)/water (2 mL) mixture in a microwave test tube (15 mL). The required amount of catalyst (0.3, 0.03, or 0.007 mol % Pd) was

https://dx.doi.org/10.1021/acsami.0c03331
ACS Appl. Mater. Interfaces 2020, 12, 23844−23852

dispersed, followed by the addition of 133 mg of K_2CO_3 (0.96 mmol, 3 equiv) in the test tube (15 mL). The test tube was then placed in a microwave reaction chamber, stirred, and heated to 60 °C for 5 min. The reactants and products were collected by ethyl acetate and separated by centrifugation. The reaction progress was monitored by GC-FID.

2.6. Procedure for Recycling the Pd/TiO_2 Catalyst for Suzuki Coupling Reaction by MWI. The required amount of the Pd/TiO_2 catalyst was added in an ethanol (2 mL)/water (2 mL) mixture in a microwave reaction test tube (15 mL). To this test tube, 50 mg of bromobenzene (0.32 mmol, 1 equiv) and 47 mg of phenylboronic acid (0.38 mmol, 1.2 equiv) were added. Just before the start of reaction, 133 mg of K_2CO_3 (0.96 mmol, 3 equiv) was added into the test tube. The test tube was then placed in a microwave reaction chamber and stirred at 60 °C for 10 min. After completion of the reaction, a small aliquot of the solution was collected and analyzed by GC-FID. The solution was centrifuged, and the solid was collected and washed two times with DI water and two times with ethanol before it was dried in an oven at 80 °C overnight. Before using the catalyst for another run of reaction, a small amount was analyzed using inductively coupled plasma-optical emission spectroscopy (ICP-OES) to determine the Pd content in the used catalyst.

2.7. Procedure for the Synthesis of Different Biphenyl Products by Coupling Reactions under MWI. Different derivatives of the Suzuki coupling reactions were evaluated under microwave heating. Aryl bromide (0.32 mmol) was added to an ethanol (2 mL)/water (2 mL) mixture in a microwave test tube (15 mL). To this, 0.38 mmol of arylboronic acid was added along with the catalyst containing 0.3 mol % Pd. Finally, 0.96 mmol of K_2CO_3 was added to the test tube before capping the test tube. The test tube was then placed in a microwave reaction chamber and stirred at 60 °C for 10 min. The reactants and products were extracted by ethyl acetate and centrifugation. The reaction was monitored by GC-MS, and GC-FID was used to determine the % conversion.

3. RESULTS AND DISCUSSION

3.1. Catalyst Design and Synthesis. Figure 1a,b illustrates the general steps used for the synthesis of Pd nanoparticles incorporated within the metal oxide supports. The LVCC method to synthesize the metal oxide supports is schematically described in Figure 1a.[13,28−31] As described previously, the process involves laser vaporization of a metal or a semiconductor target placed on the heated lower plate (50 °C) of the LVCC chamber and separated from the cold upper plate (−60 °C) by a glass ring.[28−31] The chamber is filled with an 800−1100 Torr carrier gas mixture containing 50% O_2 in He (99.999% pure). The second harmonic of a Nd:YAG laser (λ = 532 nm, pulse width τ = 7 ns, repetition rate = 30 Hz, 70−100 mJ/pulse, Spectra Physics LAB-170-30) is used for laser vaporization, which results in the release of metal atoms (about 10^{14} atoms per laser pulse) into the gas phase.[28−31] Following the nanosecond laser pulse, the released metal atoms undergo nucleation and reactions with O_2, resulting in the formation of the oxide nanoparticles that are carried out by the gas convection and deposited on the cold top plate of the LVCC chamber.[28−31]

The key factor for the formation of small Pd nanocatalysts supported on the oxide nanoparticles is the rapid laser reduction of the Pd ions adsorbed on the oxide support by pulsed laser irradiation in an aqueous solution (LIS).[13,32,33] The LIS process provides a green, nontoxic, room-temperature, photoassisted reduction method without the need for chemical reducing agents or capping agents. Laser irradiation (532 nm, 4 W, 30 Hz) of the K_2PdCl_6 salt adsorbed on the LVCC oxide nanoparticles dispersed in an ethanol−water mixture generates $^{\bullet}C_2H_4OH$ radicals, which act as a reducing agent of the Pd ions, leading to the deposition of Pd nanoparticles on the surface of the oxide support.[13,32,33]

For a comparison with the LIS method, microwave (MW)-assisted chemical reduction using hydrazine hydrate as a reducing agent is also used for the deposition of Pd nanoparticle catalysts on the LVCC oxide supports. The characterization and properties of the Pd catalysts prepared by the LIS/LVCC and MW/LVCC methods are described and compared below.

3.2. Catalyst Characterization and Properties. Figure 2a−d displays the X-ray diffraction (XRD) patterns of the

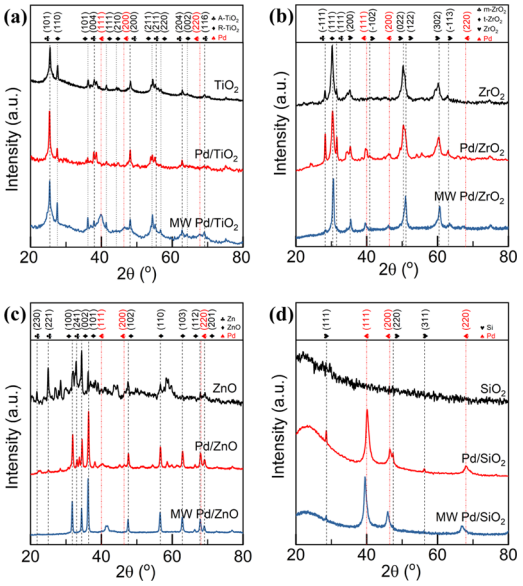

Figure 2. XRD patterns for (a) TiO_2 (black), LIS-Pd/TiO_2 (red), and MW-Pd/TiO_2 (blue); (b) ZrO_2 (black), LIS-Pd/ZrO_2 (red), and MW-Pd/ZrO_2 (blue); (c) ZnO (black), LIS-Pd/ZnO (red), and MW-Pd/ZnO (blue); and (d) SiO_2 (black), LIS-Pd/SiO_2 (red), and MW- Pd/SiO_2 (blue).

LVCC oxide supports TiO_2, ZrO_2, ZnO, and SiO_2, respectively (black patterns), along with the oxide-supported Pd catalysts prepared by the LIS/LVCC (red patterns) and the MW/LVCC (blue patterns) methods. As shown in Figure 2a, the LVCC-TiO_2 nanoparticles exhibit mostly the anatase phase (JCPDS ref # 21-1272) with a small amount of the rutile phase (JCPDS ref # 21-1276). Based on the relative intensities of the diffraction peaks characteristic of the anatase phase at 2θ = 26, 38, 48, 54, and 55°, it can be concluded that the LVCC-TiO_2 support contains ∼90 and ∼10% anatase and rutile phases, respectively.[34,35] It is suspected that in such a mixed phase oxide, interstitials and oxygen vacancies are present, especially at the interface between the two phases.[34,35] Figure 2a also shows that the LIS-Pd/TiO_2 catalyst does not display the characteristic (111) Pd diffraction at 2θ = ∼40°, which indicates small well-dispersed Pd nanoparticles within the TiO_2 support.[36] However, this Pd peak is clearly visible in the XRD pattern of the MW-Pd/TiO_2 catalyst, indicating that larger Pd nanoparticles are deposited by the MW-assisted chemical reduction method. Interestingly, the Pd diffraction peak is also observed in the LIS-deposited catalysts on the ZnO, ZrO_2, and SiO_2 supports. This may suggest that photoexcitation of the anatase−rutile mixed phase could be involved in the photoreduction of the Pd ions, resulting in the nucleation of very small Pd nanoparticles confined within the oxygen

https://dx.doi.org/10.1021/acsami.0c03331
ACS Appl. Mater. Interfaces 2020, 12, 23844−23852

vacancies of the TiO_2 support. It is also noted that in the case of the ZnO support, the Pd peak is significantly smaller than in the ZrO_2- and SiO_2-supported catalysts, which could suggest a stronger catalyst−support interaction in the Pd/ZnO catalyst than in the Pd/ZrO_2 and Pd/SiO_2 catalysts. In fact, the strongest Pd diffraction peaks are observed for the catalysts deposited on the SiO_2 support (Figure 2d) by both the LIS and the MW methods. This indicates that the Pd/SiO_2 catalysts are expected to have larger and aggregated Pd nanoparticles and consequently less catalytic activity. Another important result from the data shown in Figure 2 is that the structural integrity of the four oxide supports remains intact after the deposition of the Pd nanoparticles by either the LIS or the MW reduction method. This is expected based on the low temperatures (nearly room temperature) used in both the reduction methods.

X-ray photoelectron spectroscopy (XPS) is used to examine the surface chemical composition and valence electronic states of the oxide supports. The XPS survey scans corresponding to the four LVCC supports are shown in Figure S1 (Supporting Information). The O/Ti, O/Zr, O/Zn, and O/Si atomic ratios are calculated from the XPS data as 1.92, 1.93, 0.8, and 5.1, respectively. The high O/Si ratio in SiO_2 is due to the presence of the unsaturated surface valences on the silica surface that can be saturated by the chemisorption of water, leading to the formation of covalently bonded surface hydroxyl groups (silanol).[37] However, the unusually low stoichiometric ratios of O/Ti, O/Zr, and O/Zn indicate that these oxide supports synthesized by the LVCC are substoichiometric, consistent with previous LVCC results.[28,29,31] The substoichiometric TiO_{2-x}, ZrO_{2-y}, and ZnO_{1-z} oxides could provide available sites for the nucleation of small Pd nanoparticles following the photoreduction of the Pd ions by the LIS method.[13] This is consistent with the lack of the Pd diffraction peaks in the XRD pattern of the LIS-Pd/TiO_2 catalyst (Figure 2a).

The Ti 2p, Zr 3d, Zn 2p, and Si 2p XPS spectra of the LIS-Pd/TiO_2, LIS-Pd/ZrO_2, LIS-Pd/ZnO, and LIS-Pd/SiO_2 catalysts (Figure S2, Supporting Information) indicate 100% of the Ti^{4+}, Zr^{4+}, Zn^{2+}, and Si^{4+} states, respectively, thus confirming that all of the supports consist only of oxides and no metallic species (Ti^0, Zr^0, Zn^0, or Si^0) are present. Although the LVCC method can result in the formation of both metallic and oxide nanoparticles, the metallic nanoparticles are readily oxidized during the LIS process.[13,33]

To identify the electronic states of the Pd nanocatalysts incorporated within the four supports by the LIS method, the binding energies of the Pd 3d electrons are measured and the XPS spectra are shown in Figure 3. The results show the appearance of the $Pd_{5/2}$ and $Pd_{3/2}$ fitted peaks at ~335 and ~340 eV, respectively,[13,15,38] indicating the presence of Pd^0 with 75, 100, 65, and 91% in the catalysts deposited on the TiO_2, ZrO_2, ZnO, and SiO_2 supports, respectively. Therefore, the LIS method is capable of depositing high contents of Pd^0 on the oxide support, irrespective of the support type. Similarly, the MW-deposited Pd catalysts show high percentages of Pd^0 reaching 80, 100, 100, and 71% in the MW-Pd/TiO_2, MW-Pd/ZrO_2, MW-Pd/ZnO, and MW-Pd/SiO_2 catalysts, respectively (Figure S3, Supporting Information). It is well established that the high activity of the Pd catalysts in cross-coupling reactions correlates with the high content of Pd^0, which is required to initialize the catalytic cycle.[3,4] However, other factors such as the Pd particle size and

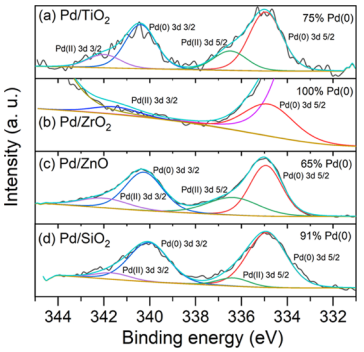

Figure 3. Pd 3d XPS of the Pd catalysts deposited by the LIS method: (a) Pd/TiO_2, (b) Pd/ZrO_2, (c) Pd/ZnO, and (d) Pd/SiO_2.

catalyst−support interaction are also critical in determining the catalytic activity and recyclability of the catalyst.[3,4]

The surface areas of the oxide supports are determined by N_2 adsorption−desorption measurements at 77 K, as shown in Figure S4 (Supporting Information), which displays the measured isotherms for the four supports. The Brunauer−Emmett−Teller (BET) specific surface areas of the TiO_2, ZrO_2, ZnO, and SiO_2 LVCC oxide supports are determined to be 130, 23, 38, and 360 m^2/g, respectively. The high surface area of the LVCC SiO_2 support is consistent with the high O/Si atomic ratio (5.1) determined by XPS and is attributed to the chemisorption of water, leading to the formation of covalently bonded surface hydroxyl groups.[37]

The morphologies of the LVCC oxide supports are analyzed by transmission electron microscopy (TEM), as shown in Figure 4. Both TiO_2 and ZrO_2 have small particle sizes of 7.5 ±

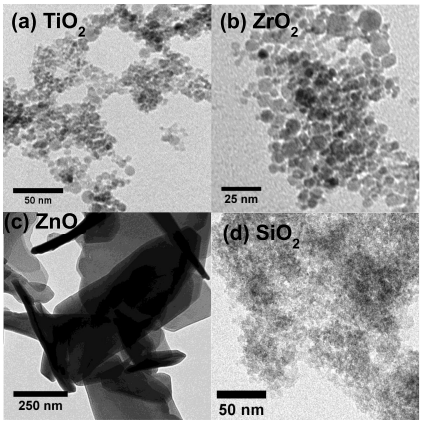

Figure 4. TEM images for LVCC-synthesized oxide supports: (a) TiO_2, (b) ZrO_2, (c) ZnO, and (d) SiO_2.

2.0 and 5.8 ± 2.8 nm, respectively, and exhibit the weblike structure morphology characteristic of the nanoparticles formed by the LVCC method.[28,29,31] The SiO_2 also shows a homogeneous distribution of ultrasmall particles, although accurate particle size distribution could not be determined using the current TEM resolution. The ZnO particles exhibit larger sizes and display both sheet- and rodlike morphologies.

Figure 5a,b displays TEM images of the LIS- and MW-deposited Pd catalysts, respectively, on the LVCC oxide supports. The Pd particle size distributions are shown in Figure S5a,b, Supporting Information. For the LIS method, the Pd particle sizes are 5.2 ± 2.7, 7.7 ± 3.1, 5.6 ± 3.1, and 9.6 ± 5.2

https://dx.doi.org/10.1021/acsami.0c03331
ACS Appl. Mater. Interfaces 2020, 12, 23844−23852

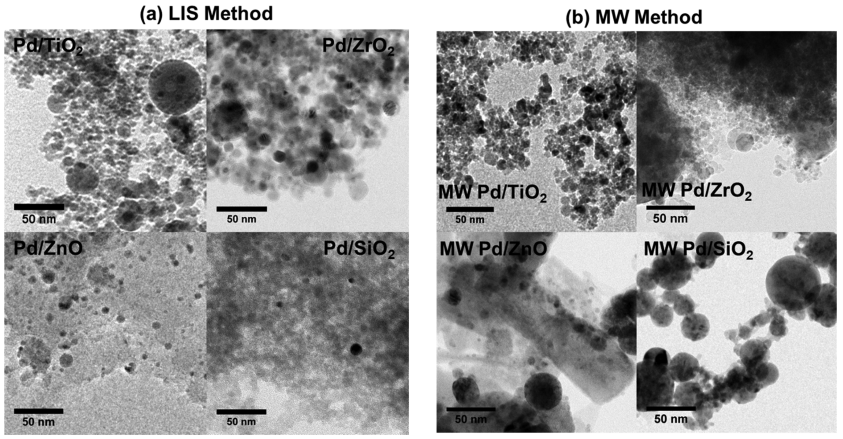

Figure 5. TEM images of the Pd nanoparticles deposited by (a) the LIS method and (b) the MW method on the oxide supports prepared by the LVCC method.

nm for the LIS-Pd/TiO_2, LIS-Pd/ZrO_2, LIS-Pd/ZnO, and LIS-Pd/SiO_2 catalysts, respectively (Figure 5a). For the MW method, the Pd particle sizes are 6.7 ± 3.6, 10.6 ± 3.9, 9.5 ± 7.1, and 26.4 ± 13.3 nm for the MW-Pd/TiO_2, MW-Pd/ZrO_2, MW-Pd/ZnO, and MW-Pd/SiO_2 catalysts, respectively (Figure 5b). These results clearly indicate that the reduction method greatly affects the size of the nanoparticles even if the same support is used in different reduction methods. The LIS method appears to result in the deposition of smaller Pd particles with a relatively narrow size distribution compared to the MW-assisted chemical reduction method. This could be due to the extent of heating in the MW method, which can lead to the agglomeration of the nanoparticles.

The TEM results shown in Figure 5 indicate that the smallest Pd particles are generated by the LIS method on the surface of the TiO_2 oxide support. It should be noted that the Pd nanoparticles are easily distinguished from the oxide particles by the very different lattice fringes, as shown in the high-resolution TEM (HRTEM) images displayed in Figure 6. The *d*-spacings in the (111) plane of the TiO_2, ZrO_2, and ZnO crystals are measured as 0.352, 0.324, and 0.283 nm, respectively, while the *d*-spacings in the Pd(111) plane are measured as 0.229, 0.228, 0.228, and 0.238 nm for the Pd/TiO_2, Pd/ZrO_2, Pd/ZnO, and Pd/SiO_2 catalysts, respectively (Figure 6). Similar values are measured for the *d*-spacing in the (111) planes of the catalysts prepared by the MW method, as shown in Figure S6 (Supporting Information).

3.3. Catalyst Evaluation and Structural Correlations.

The activities of the eight catalysts prepared by the LIS/LVCC and MW/LVCC methods are evaluated using the reaction between bromobenzene and benzeneboronic acid in an ethanol−water (1:1) solvent mixture. The reaction is conducted using the 0.3 mol % supported Pd catalyst under 5 min microwave irradiation (MWI, 300 W) at 60 °C, as described in Scheme 1. The % conversion of bromobenzene to the biphenyl product and the properties of the supported catalysts are summarized in Table 1.

The results shown in Table 1 indicate that the LIS-Pd/TiO_2 catalyst exhibits the highest catalytic activity with 92% conversion to the biphenyl product in 5 min at 60 °C. This could be attributed to the small size of Pd nanoparticles (5.2 ± 2.7 nm) and the relatively large surface area of the LVCC-TiO_2 support (130 m^2/g) in the LIS-Pd/TiO_2 catalyst. It is also clear that the activity of the LIS-Pd catalysts is generally higher than

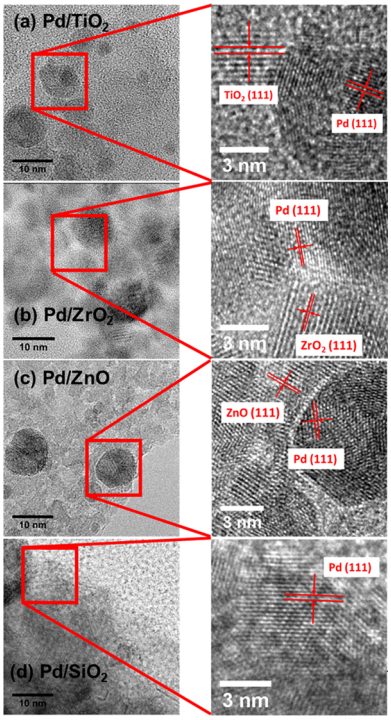

Figure 6. HRTEM images for (a) Pd/TiO_2, TiO_2(111) *d*-spacing = 0.3518 nm and Pd(111) interplanar distance = 0.2293 nm, (b) Pd/ZrO_2, ZrO_2(111) *d*-spacing = 0.3236 nm and Pd(111) interplanar distance = 0.2281 nm, (c) Pd/ZnO, ZnO(111) *d*-spacing = 0.2830 nm and Pd(111) interplanar distance = 0.2276 nm, and (d) Pd/SiO_2, Pd(111) interplanar distance = 0.2381 nm.

Scheme 1

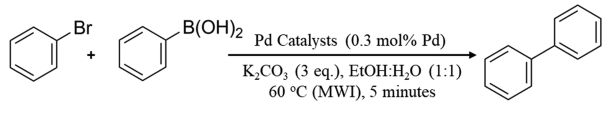

that of the MW-Pd catalysts both supported on the LVCC oxides. The increased activity of the LIS-Pd catalysts can be explained by the smaller size of the Pd nanoparticles generated by the LIS method compared to the MW-assisted chemical reduction method. The rapid laser reduction of the Pd ions adsorbed on LVCC oxides leads to the deposition of small Pd nanoparticles within the defects of the oxide support, especially

https://dx.doi.org/10.1021/acsami.0c03331
ACS Appl. Mater. Interfaces 2020, 12, 23844−23852

Table 1. Properties and Activities of the Oxide-Supported Pd Catalysts for the Suzuki Coupling Reaction

catalyst	support surface area (m^2/g)	Pd content (wt %)	Pd particle size (nm)	$Pd^{(0)}$ content (%)	% conversion MW reaction (5 min at 60 °C)
LIS-Pd/TiO_2	130	3.5	5.2 ± 2.7	75	92
LIS-Pd/ZnO	38	4.7	5.6 ± 3.1	65	83
LIS-Pd/ZrO_2	23	4.5	7.7 ± 3.1	100	29
LIS-Pd/SiO_2	360	4.3	9.6 ± 5.2	91	21
MW-Pd/TiO_2	130	3.5	6.7 ± 3.6	80	90
MW-Pd/ZnO	38	4.7	9.5 ± 7.1	71	75
MW-Pd/ZrO_2	23	4.5	10.6 ± 3.9	100	41
MW-Pd/SiO_2	360	4.3	26.4 ± 13.3	100	12

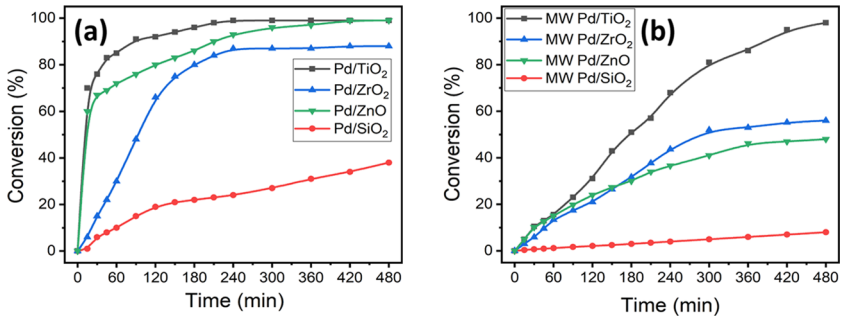

Figure 7. Conversion of bromobenzene to biphenyl as a function of reaction time at room temperature for (a) the LIS/LVCC catalysts Pd/TiO_2, Pd/ZrO_2, Pd/ZnO, and Pd/SiO_2 and (b) the MW/LVCC catalysts MW-Pd/TiO_2, MW-Pd/ZrO_2, MW-Pd/ZnO, and MW-Pd/SiO_2.

Table 2. Synthesis of Biphenyl Derivatives by Suzuki Cross-Coupling Reactions Using the LIS-Pd/TiO_2 Catalyst[a]

Aryl bromide	Aryl boronic acid	Product	Conversion (%)[b]
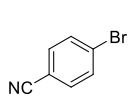	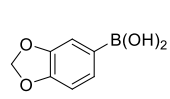	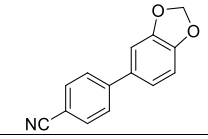	**96%**
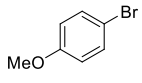	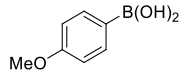	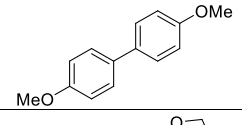	**80%**
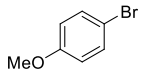	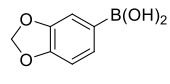	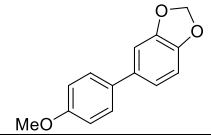	**72%**
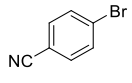	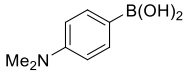	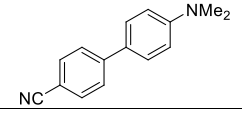	**91%**
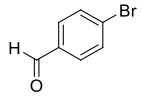	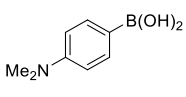	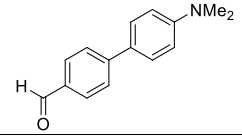	**94%**
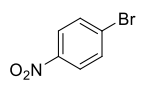	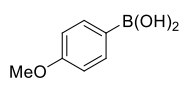	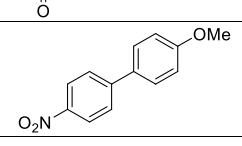	**94%**

[a]Reaction condition: aryl bromide (0.32 mmol, 1 equiv), arylboronic acid (0.38 mmol, 1.2 equiv), K_2CO_3 (0.96 mmol, 3 equiv), LIS-Pd/TiO_2 catalyst (0.3 mol % Pd), 4 mL solvent (1:1 H_2O/EtOH), reaction at 60 °C (MWI) for 10 minutes. [b]Conversion of aryl bromide (%) was determined by GC-MS and GC-FID analyses.

in the TiO_2 substoichiometric oxide. At a catalyst loading of 0.3 mol % Pd under microwave irradiation at 60 °C for 5 min, the LIS catalysts Pd/TiO_2, Pd/ZnO, and Pd/ZrO_2 are capable of converting 92, 83, and 29% of the bromobenzene to the biphenyl product, respectively. These results reveal the excellent catalytic activity of these oxide-supported Pd catalysts with turnover frequencies (TOF, h^{-1}) of 24 000, 10 000, and 3200 achieved under mirowave-assisted reactions at 60 °C for

https://dx.doi.org/10.1021/acsami.0c03331
ACS Appl. Mater. Interfaces 2020, 12, 23844−23852

the 0.03 mol% Pd/TiO_2, Pd/ZnO, and Pd/ZrO_2 catalysts, respectively. These catalytic activities are among the highest observed in Suzuki coupling reactions by Pd-supported oxide catalysts.[39−48]

To confirm and validate the efficiency of the LVCC oxide-supported Pd nanocatalysts, the Suzuki coupling reaction is also conducted at room temperature. Figure 7a,b displays the % conversion of bromobenzene to the biphenyl product as a function of reaction time for the catalysts prepared by the LIS-LVCC and MW-LVCC methods. Again, the LIS-Pd/TiO_2 catalyst displays the highest catalytic activity with 75% conversion to the biphenyl product in 15 min at room temperature compared to 60, 6, and 1% conversions for the LIS-Pd/ZnO, LIS-Pd/ZrO_2, and LIS-Pd/SiO_2 catalysts, respectively. The LIS-Pd/TiO_2 catalyst successfully converts almost 100% of bromobenzene to biphenyl within 240 min at room temperature without any heating. For comparison, the LIS-Pd/SiO_2 catalyst converts only about 24% of reactant, while the LIS-Pd/ZrO_2 and LIS-Pd/ZnO catalysts convert about 85 and 92%, respectively, after 240 min at room temperature. The room-temperature results (Figure 7a,b) also confirm the conclusion reached earlier that the activity of the LIS-Pd catalysts is generally higher than that of the MW-Pd catalysts. The increased activity of the LIS-Pd catalysts can be explained by the smaller size of the Pd nanoparticles generated by the LIS method compared to the MW-assisted chemical reduction method.

To generalize the above results, the utility of the LIS-Pd/TiO_2 catalyst is demonstrated for the synthesis of a variety of biphenyl products under microwave reaction conditions at 60 °C, and the results are shown in Table 2. The results demonstrate that a variety of biphenyl products containing electron-withdrawing groups such as nitrile, aldehyde, and nitro or electron-donating groups such as methoxy can be efficiently synthesized in high yields using the LIS-Pd/TiO_2 catalyst.

3.4. Recycling the LIS-Pd/TiO_2 Catalyst. Table 3 displays the recycling capability of the LIS-Pd/TiO_2 catalyst.

Table 3. Recycling of the Pd/TiO_2 Catalyst by the Suzuki Cross-Coupling Reaction with Pd Concentration of 0.3 mol %[a]

Run	Pd content (wt %)	Conversion (%)[b]
1	3.47	100
2	3.21	96
3	2.95	90
4	2.87	85

[a]Reaction condition: bromobenzene (0.32 mmol, 1 equiv), benzeneboronic acid (0.38 mmol, 1.2 equiv), K_2CO_3 (0.96 mmol, 3 equiv), LIS-Pd/TiO_2 catalyst (0.3 mol % Pd), 4 mL solvent (1:1 H_2O/EtOH), reaction at 60 °C (MWI) for 10 minutes. [b]Conversion of bromobenzene (%) determined by GC-FID analysis.

The spent (used) catalyst is analyzed by the ICP-OES to determine the amount of Pd present. The amount of Pd fixed at 0.3 mol % Pd is used for the subsequent runs to maintain consistency in the evaluation of the recyclability. As shown in Table 3, a conversion of more than 85% is observed for the four recycling runs performed. The amount of Pd does not decrease much after each run, indicating that the LIS-Pd/TiO_2 catalyst is stable and does not cause significant Pd leaching of the catalyst into the reaction mixture.

4. SUMMARY AND CONCLUSIONS

In this work, we have developed a new approach for the green synthesis of highly active Pd nanocatalysts supported on substoichiometric oxide nanoparticles for Suzuki cross-coupling reactions. The supports were synthesized from Ti, Zr, Zn, and Si rods using the LVCC technique in the presence of an oxygen−He gas mixture to produce substoichiometric TiO_2, ZrO_2, ZnO, and SiO_2 nanoparticles. The LVCC method generates small oxide nanoparticles with narrow particle size distributions. Structural defects such as oxygen vacancies in the nonstoichiometric oxide support enhance metal−support interaction by providing favored nucleation sites for the Pd nanoparticle catalysts. The Pd nanocatalysts are deposited on the support using laser irradiation in aqueous solutions containing the nonstoichiometric oxide support. For metal oxide supports with band gaps accessible by laser irradiation in solution, the photogenerated electrons can effectively reduce the Pd ions at room temperature without the need for chemical reducing agents, thus enabling fast and clean catalyst deposition on the surface of the support. The developed catalysts show high activity for Suzuki cross-coupling reactions between various aryl bromides and arylboronic acids. The LIS-Pd/TiO_2 catalyst with 0.3 mol % Pd achieves 100% conversion of the reactants to the biphenyl product within 240 minutes at room temperature without any external heating. With a catalyst loading of 0.3 mol % of the LIS-Pd/TiO_2 and LIS-Pd/ZnO catalysts, 92 and 83% conversions to the biphenyl product, respectively, are achieved within five minutes under microwave reaction conditions at 60 °C. The results demonstrate a remarkable catalytic activity of the substoichiometric oxide-supported Pd catalysts with turnover frequencies (TOF, h^{-1}) of 24 000, 10 000, and 3200 achieved under mirowave-assisted reactions at 60 °C for the 0.03 mol% LIS-Pd/TiO_2, LIS-Pd/ZnO, and LIS-Pd/ZrO_2 catalysts, respectively. The high activity and excellent reusability of these nanocatalysts are attributed to the strong catalyst−support interaction between the small Pd nanoparticles and the surface defects of the substoichiometric oxide support. The combined LVCC−LIS techniques presented here provide a green synthesis route of the oxide-supported Pd nanoparticle catalysts, which exhibit high activity and good reusability for carbon−carbon bond-forming reactions.

■ ASSOCIATED CONTENT

Supporting Information

The Supporting Information is available free of charge at https://pubs.acs.org/doi/10.1021/acsami.0c03331.

XPS survey scans of the substoichiometric oxide supports (Figure S1); Ti 2p, Zr 3d, Zn 2p, and Si 2p XPS after the laser deposition of the Pd nanocatalysts (Figure S2); Pd 3d XPS of the Pd catalysts deposited by the MW-assisted chemical reduction on the LVCC substoichiometric oxide supports (Figure S3); N_2 adsorption−desorption isotherms at 77 K for the oxide supports (Figure S4); Pd particle size distributions for the LIS- and MW-deposited Pd catalysts (Figure S5); and HRTEM images for MW-deposited Pd catalysts on the LVCC substoichiometric oxide supports (Figure S6) (PDF)

https://dx.doi.org/10.1021/acsami.0c03331
ACS Appl. Mater. Interfaces 2020, 12, 23844−23852

AUTHOR INFORMATION

Corresponding Author

M. Samy El-Shall − *Department of Chemistry, Virginia Commonwealth University, Richmond, Virginia 23284-2006, United States;* orcid.org/0000-0002-1013-4948; Email: mselshal@vcu.edu

Authors

Mrinmoy K. Das − *Department of Chemistry, Virginia Commonwealth University, Richmond, Virginia 23284-2006, United States*

Julian A. Bobb − *Department of Chemistry, Virginia Commonwealth University, Richmond, Virginia 23284-2006, United States*

Amr A. Ibrahim − *Department of Chemistry, Faculty of Science, Mansoura University, Al-Mansoura 35516, Egypt;* orcid.org/0000-0002-1315-6616

Andrew Lin − *Department of Chemistry, Virginia Commonwealth University, Richmond, Virginia 23284-2006, United States*

Khaled M. AbouZeid − *Department of Chemistry, Virginia Commonwealth University, Richmond, Virginia 23284-2006, United States*

Complete contact information is available at: https://pubs.acs.org/10.1021/acsami.0c03331

Notes

The authors declare no competing financial interest.

ACKNOWLEDGMENTS

The authors thank the National Science Foundation (CHE-1900094) for the support of this work. This work was also partially supported by the Center for Rational Catalysis Synthesis (CeRCaS), an Industry/University Cooperative Research Center funded in part by the National Science Foundation [Industry/University Collaborative Research Center grant IIP1464595].

REFERENCES

(1) Molnár, Á. Efficient, Selective, and Recyclable Palladium Catalysts in Carbon−Carbon Coupling Reactions. *Chem. Rev.* **2011**, *111*, 2251−2320.

(2) Suzuki, A. Cross-Coupling Reactions of Organoboranes: An Easy Way To Construct C-C Bonds (Nobel Lecture). *Angew. Chem., Int. Ed.* **2011**, *50*, 6722−6737.

(3) Seechurn, C. C. C. J.; Kitching, M. O.; Colacot, T. J.; Snieckus, V. Palladium-Catalyzed Cross-Coupling: A Historical Contextual Perspective to the 2010 Nobel Prize. *Angew. Chem., Int. Ed.* **2012**, *51*, 5062−5085.

(4) Biffis, A.; Centomo, P.; Zotto, A. D.; Zecca, M. Pd Metal Catalysts for Cross-Couplings and Related Reactions in the 21st Century : A Critical Review. *Chem. Rev.* **2018**, *118*, 2249−2295.

(5) Li, H.; Seechurn, C. C. J.; Colacot, T. J. Development of Preformed Pd Catalysts for Cross-Coupling Reactions, Beyond the 2010 Nobel Prize. *ACS Catal.* **2012**, *2*, 1147−1164.

(6) Das, P.; Linert, W. Schiff Base-derived Homogeneous and Heterogeneous Palladium Catalysts for the Suzuki−Miyaura Reaction. *Coord. Chem. Rev.* **2016**, *311*, 1−23.

(7) Fihri, A.; Bouhrara, M.; Nekoueishahraki, B.; Basset, J. M.; Polshettiwar, V. Nanocatalysts for Suzuki cross-coupling reactions. *Chem. Soc. Rev.* **2011**, *40*, 5181−5203.

(8) Zapf, A.; Beller, M. Fine Chemical Synthesis with Homogeneous Palladium Catalysts: Examples, Status and Trends. *Top. Catal.* **2002**, *19*, 101−109.

(9) Pagliaro, M.; Pandarus, V.; Ciriminna, R.; Béland, F.; Demma Carà, P. Heterogeneous versus Homogeneous Palladium Catalysts for Cross-Coupling Reactions. *ChemCatChem* **2012**, *4*, 432−445.

(10) Chemler, S. R.; Trauner, D.; Danishefsky, S. J. The B-Alkyl Suzuki−Miyaura Cross-Coupling Reaction: Development, Mechanistic Study, and Applications in Natural Product Synthesis. *Angew. Chem., Int. Ed.* **2001**, *40*, 4544−4568.

(11) Siamaki, A. R.; Khder, A. E. R. S.; Abdelsayed, V.; El-Shall, M. S.; Gupton, B. F. Microwave-Assisted Synthesis of Palladium Nanoparticles Supported on Graphene: A Highly Active and Recyclable Catalyst for Carbon-Carbon Cross-Coupling Reactions. *J. Catal.* **2011**, *279*, 1−11.

(12) Elazab, H. A.; Siamaki, A. R.; Moussa, S.; Gupton, B. F.; El-Shall, M. S. Highly Efficient and Magnetically Recyclable Graphene-Supported Pd/Fe_3O_4 Nanoparticle Catalysts for Suzuki and Heck Cross-Coupling Reactions. *Appl. Catal., A* **2015**, *491*, 58−69.

(13) Bobb, J. A.; Ibrahim, A. A.; El-Shall, M. S. Laser Synthesis of Carbonaceous TiO_2 from Metal−Organic Frameworks: Optimum Support for Pd Nanoparticles for C−C Cross-Coupling Reactions. *ACS Appl. Nano Mater.* **2018**, *1*, 4852−4862.

(14) Ibrahim, A. A.; Lin, A.; Adly, M. S.; El-Shall, M. S. Enhancement of the Catalytic Activity of Pd Nanoparticles in Suzuki Coupling by Partial Functionalization of the Reduced Graphene Oxide Support with p-Phenylenediamine and Benzidine. *J. Catal.* **2020**, *385*, 194−203.

(15) Mohan, M. K.; Sunajadevi, K. R.; Daniel, N. K.; Gopi, S.; Sugunan, S.; Perumparakunnel, N. C. Cu/Pd Bimetallic Supported on Mesoporous TiO_2 for Suzuki Coupling Reaction. *Bull. Chem. React. Eng. Catal.* **2018**, *13*, 286−294.

(16) Nasrollahzadeh, M.; Mohammad Sajadi, S. Green Synthesis, Characterization and Catalytic Activity of the Pd/TiO_2 Nanoparticles for the Ligand-Free Suzuki−Miyaura Coupling Reaction. *J. Colloid Interface Sci.* **2016**, *465*, 121−127.

(17) Wang, M.; Guo, D.; Li, H. High Activity of Novel Pd/TiO_2 Nanotube Catalysts for Methanol Electro-Oxidation. *J. Solid State Chem.* **2005**, *178*, 1996−2000.

(18) Fan, G.; Zou, B.; Cheng, S.; Zheng, L. Ligandless Palladium Supported on SiO_2−TiO_2 as Effective Catalyst for Suzuki Reaction. *J. Ind. Eng. Chem.* **2010**, *16*, 220−223.

(19) Mondal, P.; Bhanja, P.; Khatun, R.; Bhaumik, A.; Das, D.; Manirul Islam, S. Palladium Nanoparticles Embedded on Mesoporous TiO_2 Material (Pd@MTiO$_2$) as an Efficient Heterogeneous Catalyst for Suzuki-Coupling Reactions in Water Medium. *J. Colloid Interface Sci.* **2017**, *508*, 378−386.

(20) Sreedhar, B.; Yada, D.; Reddy, P. S. Nanocrystalline Titania-Supported Palladium(0) Nanoparticles for Suzuki−Miyaura Cross-Coupling of Aryl and Heteroaryl Halides. *Adv. Synth. Catal.* **2011**, *353*, 2823−2836.

(21) Monopoli, A.; Nacci, A.; Calò, V.; Ciminale, F.; Cotugno, P.; Mangone, A.; Giannossa, L. C.; Azzone, P.; Cioffi, N. Palladium/Zirconium Oxide Nanocomposite as a Highly Recyclable Catalyst for C-C Coupling Reactions in Water. *Molecules* **2010**, *15*, 4511−4525.

(22) Hosseini-Sarvari, M.; Razmi, Z. Palladium Supported on Zinc Oxide Nanoparticles as Efficient Heterogeneous Catalyst for Suzuki-Miyaura and Hiyama Reactions under Normal Laboratory Conditions. *Helv. Chim. Acta* **2015**, *98*, 805−818.

(23) Wang, P.; Liu, H.; Niu, J.; Li, R.; Ma, J. Entangled Pd Complexes over Fe_3O_4@SiO_2 as Supported Catalysts for Hydrogenation and Suzuki Reactions. *Catal. Sci. Technol.* **2014**, *4*, 1333−1339.

(24) Han, P.; Wang, X.; Qiu, X.; Ji, X.; Gao, L. One-Step Synthesis of Palladium/SBA-15 Nanocomposites and Its Catalytic Application. *J. Mol. Catal. A: Chem* **2007**, *272*, 136−141.

(25) Hajipour, A. R.; Kalantari Tarrari, M.; Jajarmi, S. Synthesis and Characterization of 4-AMTT-Pd(II) Complex over Fe_3O_4@SiO_2 as Supported Nanocatalyst for Suzuki-Miyaura and Mizoroki-Heck Cross-Coupling Reactions in Water. *Appl. Organomet. Chem.* **2018**, *32*, No. e4171.

(26) Campbell, C. T. Electronic Perturbations. *Nat. Chem.* **2012**, *4*, 597−598.
(27) Fu, J.; Yue, Q.; Guo, H.; Ma, C.; Wen, Y.; Zhang, H.; Zhang, N.; Zheng, Y.; Zheng, J.; Chen, B.-H. Constructing $Pd/CeO_2/C$ To Achieve High Leaching Resistance and Activity for Catalytic Wet Air Oxidation of Aqueous Amide. *ACS Catal.* **2018**, *8*, 4980−4985.
(28) Glaspell, G.; Anderson, J.; Wilkins, J. R.; El-Shall, M. S. Vapor Phase Synthesis of Upconverting Y_2O_3 Nanocrystals Doped with Yb^{3+}, Er^{3+}, Ho^{3+} and Tm^{3+} to Generate Red, Green, Blue and White Light. *J. Phys. Chem. C* **2008**, *112*, 11527−11531.
(29) Yang, Y.; Saoud, K. M.; Abdelsayed, V.; Glaspell, G.; Deevi, S.; El-Shall, M. S. Vapor Phase Synthesis of Supported Pd, Au and Unsupported Bimetallic Nanoparticle Catalysts for CO Oxidation. *Catal. Commun.* **2006**, *7*, 281−284.
(30) El-Shall, M. S.; Abdelsayed, V.; Pithawalla, Y. B.; Alsharach, E.; Deevi, S. C. Vapor Phase Growth and Assembly of Metallic, Intermetallic, Carbon, and Silicon Nanoparticle Filaments. *J. Phys. Chem. B* **2003**, *107*, 2882−2886.
(31) El-Shall, M. S.; Slack, W.; Vann, W.; Kane, D.; Hanley, D. Synthesis of Nanoscale Metal Oxide Particles Using Laser Vaporization/Condensation in a Diffusion Cloud Chamber. *J. Phys. Chem. A.* **1994**, *98*, 3067−3070.
(32) Rodrigues, C. J.; Bobb, J. A.; John, M. G.; Fisenko, S. P.; El-Shall, M. S.; Tibbetts, K. M. Nucleation and Growth of Gold Nanoparticles Initiated by Nanosecond and Femtosecond Laser Irradiation of Aqueous $[AuCl_4]^-$. *Phys. Chem. Chem. Phys.* **2018**, *20*, 28465−28475.
(33) Moussa, S.; Abdelsayed, V.; El-Shall, M. S. Laser Synthesis of Pt, Pd, CoO and Pd−CoO Nanoparticle Catalysts Supported on Graphene. *Chem. Phys. Lett.* **2011**, *510*, 179−184.
(34) Dambournet, D.; Belharouak, I.; Amine, K. Tailored Preparation Methods of TiO2 Anatase, Rutile, Brookite: Mechanism of Formation and Electrochemical Properties. *Chem. Mater.* **2010**, *22*, 1173−1179.
(35) Kawahara, T.; Konishi, Y.; Tada, H.; Tohge, N.; Nishii, J.; Ito, S. A Patterned TiO_2 (Anatase)/TiO_2 (Rutile) Bilayer-Type Photocatalyst: Effect of the Anatase/Rutile Junction on the Photocatalytic Activity. *Angew. Chem., Int. Ed.* **2002**, *41*, 2811−2813.
(36) Wang, M.; Guo, D.; Li, H. High Activity of Novel Pd/TiO_2 Nanotube Catalysts for Methanol Electro-Oxidation. *J. Solid State Chem.* **2005**, *178*, 1996−2000.
(37) Zhuravlev, L. T. Concentration of Hydroxyl Groups on the Surface of Amorphous Silica. *Langmuir* **1987**, *3*, 316−318.
(38) Moussa, S.; Siamaki, A. R.; Gupton, B. F.; El-Shall, M. S. Pd-Partially Reduced Graphene Oxide Catalysts (Pd/PRGO): Laser Synthesis of Pd Nanoparticles Supported on PRGO Nanosheets for Carbon−Carbon Cross Coupling Reactions. *ACS Catal.* **2012**, *2*, 145−154.
(39) Razavi, N.; Akhlaghinia, B.; Jahanshahi, R. Aminophosphine Palladium(0) Complex Supported on ZrO_2 Nanoparticles (ZrO_2@AEPH2-PPh2-Pd(0)) as an Efficient Heterogeneous Catalyst for Suzuki−Miyaura and Heck−Mizoroki Reactions in Green Media. *Catal. Lett.* **2017**, *147*, 360−373.
(40) Feizpour, F.; Jafarpour, M.; Rezaeifard, A. Band Gap Modification of TiO_2 Nanoparticles by Ascorbic Acid-Stabilized Pd Nanoparticles for Photocatalytic Suzuki−Miyaura and Ullmann Coupling Reactions. *Catal. Lett.* **2019**, *149*, 1595−1610.
(41) Farzad, E.; Veisi, H. Fe_3O4/SiO_2 Nanoparticles Coated with Polydopamine as a Novel Magnetite Reductant and Stabilizer Sorbent for Palladium Ions: Synthetic Application of Fe_3O_4/SiO_2@PDA/Pd for Reduction of 4-Nitrophenol and Suzuki Reactions. *J. Ind. Eng. Chem.* **2018**, *60*, 114−124.
(42) Kamari, Y.; Ghiaci, M. Incorporation of TiO2 Coating on a Palladium Heterogeneous Nanocatalyst. A New Method to Improve Reusability of a Catalyst. *Catal. Commun.* **2016**, *84*, 16−20.
(43) Heidari, F.; Hekmati, M.; Veisi, H. Magnetically Separable and Recyclable Fe3O4@SiO2/Isoniazide/Pd Nanocatalyst for Highly Efficient Synthesis of Biaryls by Suzuki Coupling Reactions. *J. Colloid Interface Sci.* **2017**, *501*, 175−184.
(44) Bankar, D. B.; Hawaldar, R. R.; Arbuj, S. S.; Shinde, S. T.; Gadde, J. R.; Rakshe, D. S.; Amalnerkar, D. P.; Kanade, K. G. Palladium Loaded on ZnO Nanoparticles: Synthesis, Characterization and Application as Heterogeneous Catalyst for Suzuki−Miyaura Cross-Coupling Reactions under Ambient and Ligand-Free Conditions. *Mater. Chem. Phys.* **2020**, *243*, No. 122561.
(45) Jadhav, S.; Jagdale, A.; Kamble, S.; Kumbhar, A.; Salunkhe, R. Palladium Nanoparticles Supported on a Titanium Dioxide Cellulose Composite (PdNPs@TiO_2 −Cell) for Ligand-Free Carbon−Carbon Cross Coupling Reactions. *RSC Adv.* **2016**, *6*, 3406−3420.
(46) Veisi, H.; Kamangar, S. A.; Mohammadi, P.; Hemmati, S. Palladium Nanoparticles-Decorated Triethanolammonium Chloride Ionic Liquid-Modified TiO_2 Nanoparticles (TiO_2/IL-Pd): A Highly Active and Recoverable Catalyst for Suzuki−Miyaura Cross-Coupling Reaction in Aqueous Medium. *Appl. Organomet. Chem.* **2019**, *33*, No. e4909.
(47) Wang, J.; Bai, J.; Liang, H.; Li, C. Photothermal Catalytic Effect of Pd-TiO_2/CNFs Composite Catalyst in Suzuki Coupling Reaction. *Colloids Surf., A* **2019**, *572*, 283−289.
(48) Hosseini-Sarvari, M.; Bazyar, Z. Visible Light Driven Photocatalytic Cross-Coupling Reactions on Nano Pd/ZnO Photocatalyst at Room-Temperature. *ChemistrySelect* **2018**, *3*, 1898−1907.

https://dx.doi.org/10.1021/acsami.0c03331
ACS Appl. Mater. Interfaces 2020, 12, 23844−23852